Showcasing research from Professor Robert Vícha's laboratory, Department of Chemistry, Faculty of Technology, Tomas Bata University in Zlín, Czech Republic.

Allosteric release of cucurbit[6]uril from a rotaxane using a molecular signal

Rotaxanes can be viewed as a reservoir for their macrocyclic components. However, to achieve this, it is necessary to find a way to release the previously mechanically bound macrocycle, ideally in a manner that preserves the molecular integrity of all components of the original rotaxane. We have discovered a way to exploit the repulsive electrostatic interactions between the portals of cucurbit[n]urils for this function. The surprising finding is that the repulsive inter-portal interactions are strong enough to enable the macrocyclic component of the original rotaxane to overcome the barrier of mechanical binding.

Artwork by Anna Mráčková.

As featured in:

See Robert Vícha *et al.*, *Chem. Sci.*, 2025, **16**, 83.

ROYAL SOCIETY OF CHEMISTRY

15 YEARS ANNIVERSARY

rsc.li/chemical-science

Chemical Science

ROYAL SOCIETY OF CHEMISTRY

EDGE ARTICLE

View Article Online
View Journal | View Issue

Cite this: *Chem. Sci.*, 2025, **16**, 83

All publication charges for this article have been paid for by the Royal Society of Chemistry

Received 18th June 2024
Accepted 31st October 2024

DOI: 10.1039/d4sc03970j

rsc.li/chemical-science

Allosteric release of cucurbit[6]uril from a rotaxane using a molecular signal†

Aneta Závodná, [a] Petr Janovský, [a] Václav Kolařík, [a] Jas S. Ward, [b] Zdeňka Prucková, [a] Michal Rouchal, [a] Kari Rissanen [b] and Robert Vícha *[a]

Rotaxanes can be regarded as storage systems for their wheel components, which broadens their application potential as a complement to the supramolecular systems that retain a mechanically interlocked structure. However, utilising rotaxanes in this way requires a method to release the wheel while preserving the integrity of all molecular constituents. Herein, we present simple rotaxanes based on cucurbit[6]uril (CB6), with an axis equipped with an additional binding motif that enables the binding of another macrocycle, cucurbit[7]uril (CB7). We demonstrate that the driving force behind the wheel dethreading originates from the binding of the signalling macrocycle to the allosteric site, leading to an increase in the system's strain. Consequently, the CB6 wheel leaves the rotaxane station overcoming the mechanical barrier. Portal–portal repulsive interactions between the two cucurbituril units play a crucial role in this process. Thus, the repulsive strength and the related rate of slipping off can be finely tuned by the length of the allosteric binding motif. Finally, we show that the CB6 wheel can be utilised within complexes with other guests in the mixture once released from the rotaxane.

Introduction

Rotaxanes represent a classical family of mechanically interlocked supramolecular systems,[1] alongside catenanes,[2] molecular knots,[3] Borromean rings,[4] and suitanes.[5] Since their very first synthesis almost sixty years ago,[6] rotaxanes have been employed as key components of molecular machines,[7] catalytic devices,[8] responsive materials,[9] drug delivery systems,[10] and molecular memories.[7a,11] Hand in hand with an increasing number of applications, various methods for rotaxane synthesis have been developed.[12] In terms of the way the building blocks are transformed to more complex architectures, there are three distinguishable approaches: threading the axle into the wheel component (slipping),[13] creating one of the components within the rotaxane (capping,[14] clipping[15]), and manipulating the size of the components (shrinking the wheel,[16] swelling the axle termini[17]). Syntheses can be performed under statistical control, using molecular recognition (including a passive metal template) or the state-of-the-art active metal template methodologies, which employ a mechanistically distinct approach in this context.[18]

Within mechanically interlocked structures, two classes can be distinguished based on whether it is topologically necessary to break a covalent bond for the system to disassemble (*e.g.* catenanes) or not (*e.g.* rotaxanes). Rotaxanes and pseudorotaxanes are topologically identical systems, with the distinction that the latter can be disassembled under suitable conditions without breaking or significantly distorting the covalent bonds. The somewhat unclear boundary between them[19] is represented by kinetically highly stable pseudorotaxanes, which, under certain conditions, are functionally equivalent to rotaxanes. Since our compounds **6a–6e** exhibit high kinetic stability at temperatures relevant for their potential applications, we will refer to them as rotaxanes in this article. Regardless, rotaxanes can be considered storage devices for their wheel components, which can be released on demand. Indeed, methods for overcoming the mechanical barrier are required for this purpose. The most common approaches to releasing a wheel from the rotaxane are to destroy an axle or remove the stopping moiety.[20] Unlike these destructive methods, the disassembly of rotaxanes into their intact molecular components is less frequently reported. In addition to dissociation by mechanical force,[21] the recent procedures follow reverse synthetic approaches. The simple inversion of the slipping process requires a high temperature and a suitable competitor to prevent the wheel from remaining at the rotaxane station. As high temperatures are incompatible with many application areas (*e.g.* biosystems either *in vitro* or *in vivo*), some systems operating at ambient

[a]*Department of Chemistry, Faculty of Technology, Tomas Bata University in Zlín, Vavrečkova 5669, 760 01 Zlín, Czech Republic. E-mail: rvicha@utb.cz*

[b]*Department of Chemistry, University of Jyväskylä, P.O. Box 35, Survontie 9 B, 40014 Jyväskylä, Finland*

† Electronic supplementary information (ESI) available: Single-crystal XRD data (CIF), experimental procedures, characterisation data, *K* values and their determination *via* ITC and ^{1}H NMR spectroscopy. CCDC 2312915–2312918. For ESI and crystallographic data in CIF or other electronic format see DOI: https://doi.org/10.1039/d4sc03970j

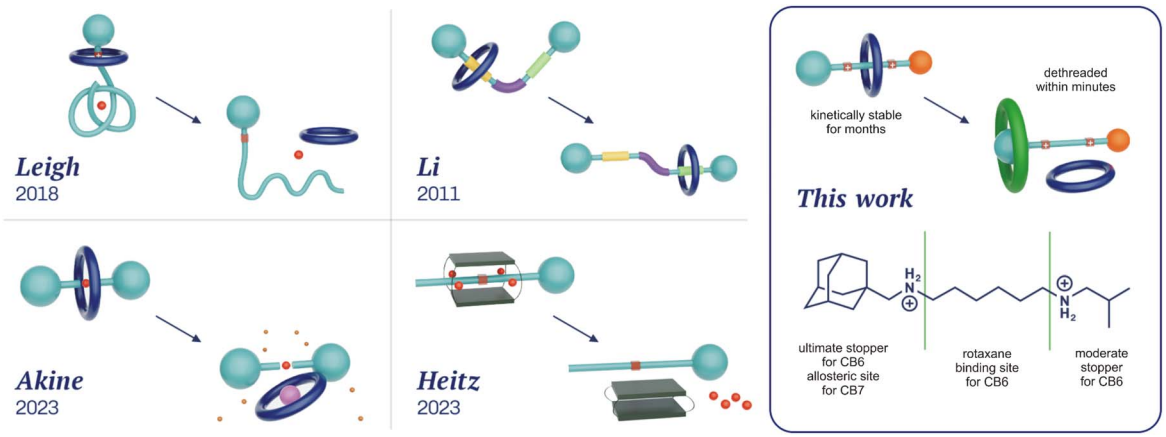

Fig. 1 Previously published approaches for wheel dethreading and the design of our new system.

temperatures have been developed (Fig. 1). Leigh and co-workers reported the removal of the crown-ether wheel *via* pH changes in conjunction with the untying of the molecular knot, reducing the bulkiness of the stopper.[22] Similarly, Li and co-workers modulated the speed of wheel slippage *via* conformational changes of H-bonded arylamide foldamers.[23] Akine and co-workers utilised the dynamic nature of palladium complexes to accelerate 27-crown-9 removal from the metallorotaxane *via* the addition of bromide as an accelerator and caesium as a competitor for 27C9 (reverse capping).[24] Finally, Heitz and co-workers inverted the shrinking process to remove a bis-porphyrin cage from its semirotaxane by the allosteric action of Ag^+ ions.[25]

Herein, we report a very simple approach for the release of the CB6 wheel by a stimulus that is orthogonal to the preparation of the rotaxane. We employed the extraordinary selectivity of cucurbit[*n*]urils (CB*n*s)[26] to arrange a system in which the originally favoured rotaxane site is no longer attractive for CB6 after the addition of CB7. CB7 strongly prefers the allosteric binding site and increases the strain of the system *via* portal–portal electrostatic repulsion, producing a metastable structure that relaxes by releasing the CB6 unit. This process inherently does not require structural changes of any component, nor any other additives (*e.g.* competitors).

Results and discussion

Structure justification and preparation of rotaxanes

We combined three previously published pieces of information in designing the axle component for our systems. First, Mock reported that the hexamethylene diammonium motif is an ideal binding site for CB6 ($K = 2.9 \times 10^8$ M^{-1}; 50 mM NaCl; 25 °C).[27] Hereinafter, we will abbreviate hexamethylene diamine/diammonium as HMDA and related binding sites as HM. Second, Masson recognised an isobutyl (IB) stopper as a kinetic barrier of 121 kJ mol^{-1}, allowing for CB6 to slip on at 120 °C while maintaining the system in a rotaxane manner at 30 °C.[13a] Third, it has been previously reported that CBn units repel each other *via* portal–portal electrostatic interactions.[28] This results in the unlikely binding of two CB*n* portals to a single cationic moiety.

Further, we used adamantane-derived motifs, which provide two functionalities. As the adamantane cage is too bulky to pass through the CB6 cavity, it serves as an ultimate stopper for this macrocycle. In contrast, the adamantane cage perfectly fits the interior of CB7 to provide an allosteric binding site with an exceptionally high affinity towards CB7. The binding strength of CB7 at adamantane-derived ammonium motifs can be modulated by the distance between the adamantane cage and the cationic moiety: the greater the distance, the weaker the complex.[29] Indeed, the greater distance decreases the repulsion between the two CB*n* units, which is crucial for expelling CB6 from its rotaxane position. Doubt arose as to whether it is possible to balance these two effects so that CB6 is released at room temperature. Therefore, we prepared a series of five rotaxanes, **6a–6e**, with variable allosteric binding motifs, as shown in Scheme 1.

The axles were synthesised from hexamethylenediamine (HMDA, **1**) *via* a sequence of Boc-protection, condensation with isobutyric aldehyde **7f**, deprotection, and second condensation with adamantane-derived aldehydes **7a–7e**. The final rotaxanes were prepared by slipping CB6 in water at 120 °C under microwave irradiation, with an overall yield of 7–14% with respect to the HMDA. Synthetic protocols and spectral characterisation for all intermediates and final rotaxanes **6a–6e** are

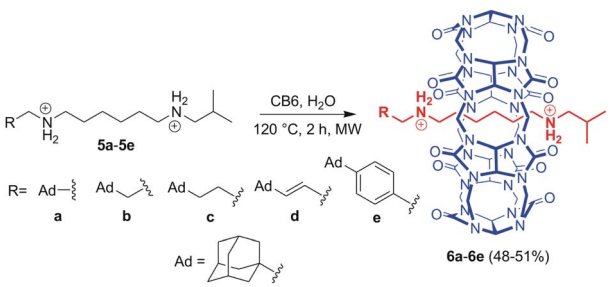

Scheme 1 Synthesis of rotaxanes **6a–6e**. Counterion chlorides are omitted for clarity.

detailed in the SI (for ^{1}H and ^{13}C NMR spectra, see Fig. S1–S20;† for ESI-MS spectra, see Fig. S21–S30†). We succeeded in growing single crystals of **6a–6d** to confirm the positioning of the CB6 unit at the HM binding site by X-ray diffraction analysis.[30] It is worth noting that the CB6 unit, although sitting on the central HM site, is slightly shifted towards the Ad terminus in all four analysed structures. The magnitude of the shifting is given in Fig. 2 as the distance Δ between the respective CB6 and HM centres of gravity. Molecular models and further details are provided in Fig. 2, S60–S63 and Table S2.†

As the rate of the slipping-on/off process depends on kinetic barriers, we initially thoroughly tested whether the complexes **6a–6e** can be considered as rotaxanes, *i.e.* determining whether the dethreading is negligible at room temperature. We prepared a mixture of **6a** (0.97 mM) with 1 equivalent of spermine·4HCl (hereinafter referred to as SP; $K_{CB6} = 3.3 \times 10^{9}$ M^{-1}, 50 mM NaCl, 25 °C)[27b] and monitored it using ^{1}H NMR spectroscopy stored at room temperature. The binding strength of CB6 at the HM site within the rotaxanes could be assumed to be similar to that of HMDA itself. Thus, considering the affinities of CB6 towards HMDA and SP, approximately 90% of CB6 should be bound at SP in the thermodynamically equilibrated mixture of **5a**, SP, and CB6 (1 : 1 : 1). However, we did not observe any changes in the NMR spectrum within ten months (Fig. S59†). Additionally, the complex **5a**@CB6^{HM} (*i.e.* **6a**) was not observed in the mixture of **6a** (or **5a** and CB6) and SP at 120 °C, implying that a kinetic barrier indeed prevents the dethreading of CB6 at 25 °C. Therefore, we consider the structures **6a–6e** as kinetically interlocked rotaxanes at room temperature. Subsequently, we tested whether CB7 was able to unlock the rotaxane barrier.

Allosteric triggering of the CB6 slipping off

The representative NMR spectra demonstrating the action of CB7 on rotaxane **6a** are shown in Fig. 3. As can be seen, two new sets of signals appeared after the addition of 1 equivalent of CB7 into a 0.85 mM solution of **6a** in D_2O at 30 °C (line ii). In the first set (marked in red), H atoms at the isobutyl terminus (H_a and H_c) are deshielded, while the H atoms of the methylene group (H_j) at the adamantane terminus are shielded. In the second set (marked in blue), all these H atoms are significantly shielded. It is worth noting that all H atoms of the adamantane cage are substantially shielded in both new sets of signals. Whereas the first set disappeared within approximately 4 hours, the second set predominated, representing 90% of the axle **5a**. It is well known that H atoms positioned inside the CB*n* cavity are strongly shielded, while there is a deshielding area outside near the portals.[26b,28a] Thus, the abovementioned data indicate that CB7 was instantly bound at the adamantane site to form a strained ternary complex[28c] **5a**@CB6^{HM},CB7^{Ad} with the CB6 unit pushed somewhat towards the IB terminus (GFN2 molecular models[31] indicate a shift of about 1.3 Å). This arrangement is not thermodynamically stable, and CB6 relatively rapidly ($t_{\frac{1}{2}} =$ 36 min) surmounts the IB stopper to form the pseudorotaxane complex **5a**@CB6^{IB},CB7^{Ad}. The mutual orientations of axle **5a**, CB7, and CB6 are represented by minimised molecular models in Fig. 3.

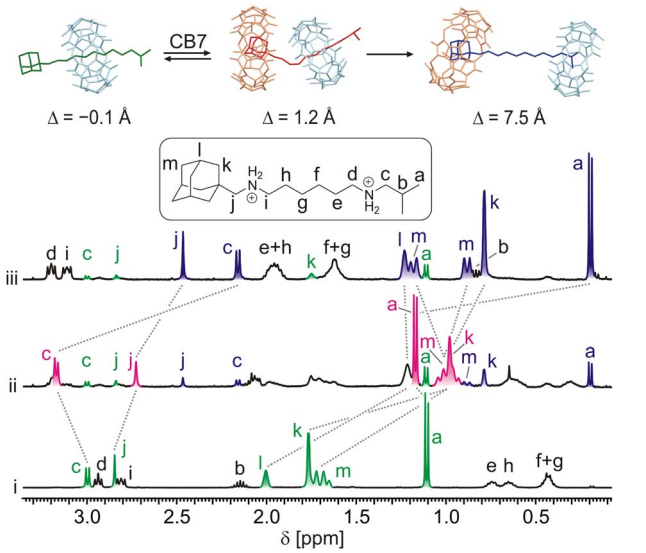

Fig. 3 Portions of ^{1}H NMR spectra (D_2O, 30 °C, 400 MHz) and molecular models (GFN2-xTB) representing observed complexes. (i) **6a** (0.85 mM); (ii) **6a** + CB7 (1 equiv.) in $t = 8$ min; (iii) **6a** + CB7 (1 equiv.) in $t = 1608$ min. Δ = distance between centres of gravity of HM site and CB6 units. Spectra are not to scale.

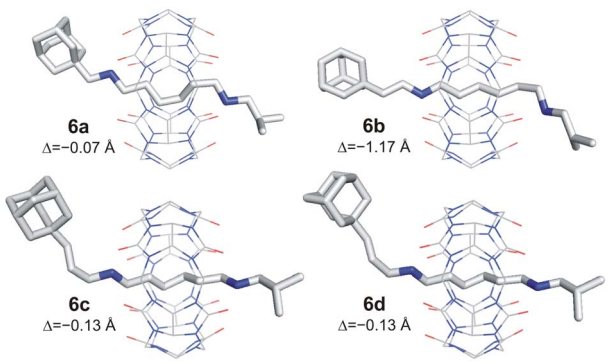

Fig. 2 X-ray structures of **6a–6d**. Minor disordered atoms, solvents, PF_6^- anions, and H-atoms are omitted for clarity. Δ = distance between centres of gravity of HM site and CB6 unit.

Continuing our study, we examined other rotaxanes **6b–6e** with CB7 to reveal how the length of the allosteric binding site influences the CB6 slipping off. The ^{1}H NMR spectra showed that CB7 was bound to Ad sites (significant shielding of Ad H atoms) and CB6 slightly moved towards the IB termini (deshielding of IB H atoms) after the addition of 1 equivalent of CB7 into solutions of rotaxanes **6b–6e** at 30 °C. However, as no other changes were observed in spectra for two months, the complexes **6b–6e**@CB7^{Ad} were considered stable at room temperature. Thus, we treated the mixtures at elevated temperatures. The rotaxanes **6b–6d** released the CB6 unit in response to the CB7 signal at 60 °C displaying respective half-lives of 1.5, 17.8, and 9.6 days (kinetic curves for all rotaxanes are given in Fig. 4A). The activation parameters obtained from the Eyring plots (Fig. 4C), along with the half-lives, are given in Table 1. It is evident that the longer the spacer between the Ad

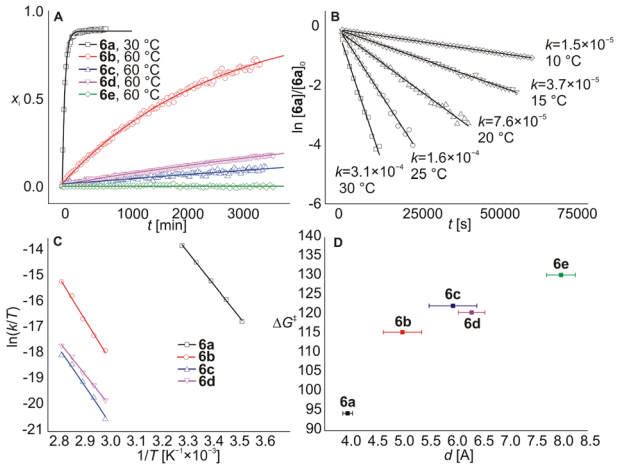

Fig. 4 The kinetic curves for decomposition of **6a–6e**@CB7 complexes (A), the first-order linearisation plot for **6a**@CB7 (B), Eyring plots for **6a–6d** (C) and the correlation plot of the allosteric binding site length *d* (obtained from molecular dynamics simulations) against the slipping-off activation energy (D).

cage and the adjacent ammonium cation, the slower the CB6 dethreading, in concert with the weaker repulsions between CB*n* portals (Fig. 4D). The inconsistency in this trend for **6c** and **6d** may be due to the fact that the ability of CB7 to occupy a specific position relative to the ammonium cation is actually more important than the mere length of the linker. Thus, even a slightly longer but sterically less bulky linker in substance **6d** may allow CB7 to approach the ammonium cation more effectively. In the case of **6e**@CB7, essentially no dethreading (<2%) was observed even at 120 °C (the temperature of rotaxane formation). This indicates that CB7 does not significantly influence the rotaxane binding site in the case of the phenylmethyl spacer, and positioning of the CB6 unit at the HM site of **5e** is thermodynamically preferred even in the presence of CB7 at the Ad terminus.

Further, we made some effort to shed light on the mechanism of the CB7 action. First, we tested the interaction of **6a** (0.83 mM) with CB7 in different ratios. Data in Fig. S55† demonstrate that the rate of the CB6 dethreading depends on the concentration of the **6a**@CB7 complex and is not affected by an excess of CB7. In addition, the kinetic data matches the first-order model, as shown for **6a**@CB7 disassembly in Fig. 4B. These experiments support our previous assumptions: the CB6 slipping off is the rate-determining step, while binding of CB7 at the allosteric Ad site is significantly faster.

Subsequently, kinetic data, along with the below-mentioned assumptions, allowed us to construct energetic profiles describing the involved supramolecular complexes and their transformations, as shown in Fig. 5. To obtain the energy gain of the first step, we determined the binding constants for the axles **5a–5e** with CB6. The *K* values given in Table S1† demonstrate that the binding strength of CB6 at the IB terminus does not depend on the nature of the allosteric Ad binding site and yields approximately 37 kJ mol^{-1}. In the second step, CB6 leaves the IB terminus and binds at the central HM station. It was found that the slipping on produced more than 95% CB6 bound at the HM site according to ^{1}H NMR spectroscopy. The kinetic barrier for this process is 121 kJ mol^{-1}, as previously determined by Masson.[13a] Thus, the barrier for the inverse slipping off must be at least about 130 kJ mol^{-1}, *i.e.* the transformation of **5**@CB6^{IB} to **6** yields about 9 kJ mol^{-1}. In the third step, the addition of CB7 and its binding at the Ad site produces **6**@CB7^{Ad} complexes. The relative energies for **6a–6d** can be determined from the activation energies of the final dethreading step, as given in Table 1. We assume that the inherent slipping-off barrier is the same for all five rotaxanes, as the nature of the allosteric Ad site does not affect the opposite terminus. The experimentally determined differences in activation energy are related to the repulsions between two CB*n* units. The affinity of the CB6 unit for the HMDA site is also weakened by the fact that it shares one ammonium cation with CB7 (the binding of two CB*n* portals to a single cationic moiety was not observed in solution).[28a,b,32] We further suppose that the slipping-on/off barriers for CB6 at **6e**@CB7^{Ad} are the same as in

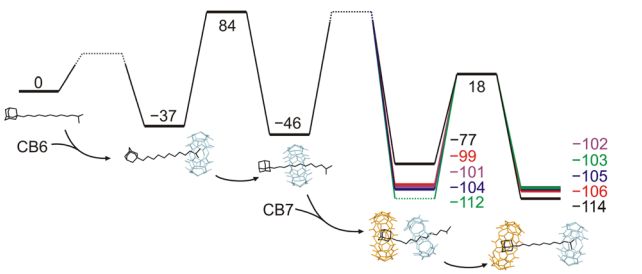

Fig. 5 A free energy profile of the transformation of the axles **5** to **5**@CB6^{IB},CB7^{Ad} through the rotaxanes **6**. Optimised models (GFN2-xTB) related to **5a** are given for illustration. **6a** (black), **6b** (red), **6c** (blue), **6d** (magenta), **6e** (green).

Table 1 Kinetic parameters of CB6 slipping off

Guest	$\Delta H^{\ddagger a}$ [kJ mol^{-1}]	$\Delta S^{\ddagger a}$ [J mol^{-1} K^{-1}]	$\Delta G^{\ddagger a}$ (30 °C) [kJ mol^{-1}]	$t_{\frac{1}{2}}{}^{b}$ (30 °C)
6a	104.9 ± 1.7	34.2 ± 0.9	94.5 ± 1.7	36.0 ± 1.4 min
6b	135 ± 6	58 ± 4	117 ± 6	200 ± 30^b d
6c	122 ± 8	−1.6 ± 0.2	122 ± 8	1500 ± 200^b d
6d	105 ± 3	−46 ± 2	119 ± 3	450 ± 30^b d
6e	na	na	≥130^c	∞

^{a} Calculated from Eyring plots. ^{b} Extrapolated from Eyring plots. ^{c} Estimated as detailed in text. na = not applicable.

the case without CB7. The final step results in complexes **5**@CB6^{IB},CB7^{Ad}, whose relative energy gains can be estimated as the superposition of binding events at both termini (respective K values are in Table S1†).

Releasing of CB6 to form other complexes

In contrast to pseudorotaxane systems that were published previously,[28c] our axles contain the terminal IB site, which binds CB6 once released from the rotaxane station. Therefore, we tested whether CB6 can be available for complexation with additional guests in the solution.

First, we prepared an equimolar mixture of rotaxane **6a** (0.68 mM) and SP, as described above, testing the stability of rotaxane. Subsequently, we added 1 equivalent of CB7 and monitored the progress by ^{1}H NMR spectroscopy (Fig. 6). Immediately after the CB7 addition, the complex SP@CB7 ($K = 4.8 \times 10^8$ M^{-1}, H_2O, 25 °C)[33] was formed almost quantitatively (with respect to CB7). The value of the association constant of CB7 at the Ad site of **6a** is not experimentally available; however, we infer that it is similar to or slightly higher than that for SP. Thus, a small portion of the strained complex **6a**@CB7^{Ad} was also observed after the CB7 addition.

As described above, this strained complex released CB6 that is subsequently captured by SP in concert with its SP/IB selectivity of approximately 6200 : 1. Even SP within the complex SP@CB7 can be taken by CB6 since the SP selectivity towards CB6/CB7 is about 3300-fold in favour of CB6. The mixture reached thermodynamic equilibrium, containing 50% of SP@CB6, 46% of **5a**@CB7, and 4% of the remaining **6a**, in 20 days. Similarly, more than 80% of CB6 was released from the original rotaxane **6a** by CB7 when HMDA was used as the final acceptor for CB6. Indeed, as the HMDA/IB selectivity of CB6 is lower than that of SP/IB, 4% of released CB6 remained bound at the IB terminus to form the **5a**@CB6^{IB},CB7^{Ad} complex (for ^{1}H NMR spectra, see Fig. S57†). The rate of the equilibration negatively correlates with the affinity of CB7 towards the competitor. Fig. S58† shows the faster equilibration for the system with SP as the thermodynamic selectivity of CB7 towards HMDA/SP is 22 : 1.

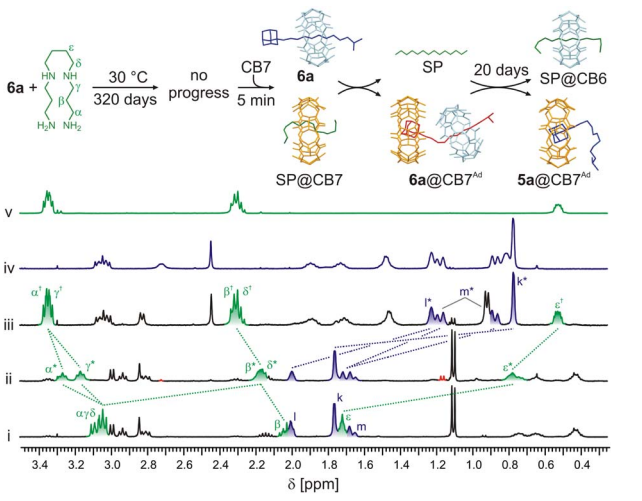

Fig. 6 Portions of ^{1}H NMR spectra (D_2O, 30 °C, 400 MHz) and molecular models (GFN2-xTB) representing observed complexes and their transformations. (i) **6a** (0.68 mM) + SP (1 equiv.); (ii) **6a** + SP + CB7 (1 equiv.) in $t = 5$ min; (iii) the same sample as previous in 20 days; (iv) **5a** (1.0 mM) + CB7 (1 equiv.); (v) SP (1.0 mM) + CB6 (1 equiv.). For signal assignment of the **6a**, see Fig. 3. The signals of the component complexed with CB6 and CB7 are labelled with † and *, respectively. Spectra are not to scale.

Conclusions

We demonstrated that steric and/or electrostatic repulsion between two cucurbit[n]uril portals arranged around a single cationic moiety is strong enough to bring a stable kinetically locked system to a dynamic state, resulting in the dethreading of the wheel. We constructed rotaxanes where the stopper moiety at one end of the axle has an additional function: it serves as an allosteric binding site with high selectivity for the trigger macrocycle. The two macrocycles, *i.e.* CB6 as the rotaxane wheel and CB7 as the trigger molecule, are known for strong electrostatic repulsion between their carbonyl-lined portals. We proved that the rotaxane with a 1-adamantylmethyl allosteric site (**6a**) is strained enough by the addition of CB7 to release CB6 at 30 °C with a half-life of 36 min. In addition, we demonstrated that the length of the allosteric binding site can be used for tuning the rate of release. Thus, ethan-1,2-diyl (**6b**), propen-1,3-diyl (**6d**) and propan-1,3-diyl (**6c**) linkers between the adamantane cage and the adjacent ammonium cation provided half-lives of 204, 451 and 1524 days at 30 °C, respectively. The CB7 unit occupying the longest 4-(1-adamantyl) benzyl moiety (**6e**) has an insignificant impact on CB6 within the rotaxane, and the complex **6e**@CB7^{Ad} is the thermodynamically preferred arrangement even at 120 °C. As the isobutyl termini of the axles represent binding site with relatively high affinity towards CB6 ($K \approx 2 \times 10^6$, 50 mM NaCl, 30 °C), CB6, once released from the rotaxane, remains bound here to form **5**@CB6^{IB},CB7^{Ad}. However, we demonstrated that CB6 is still available for complexation with other guests, *e.g.* HMDA or SP, added into the mixture.

In addition to the previously published time-dependent self-sorting systems based on cucurbiturils,[34] we present here the first example of the expulsion of the cucurbituril wheel from a rotaxane by a molecular signal. These results are particularly significant considering the high selectivity and large range of association constants of CBns, which makes them promising components of molecular devices (for example, molecular memories, catalysts or drug delivery systems).

Presently, we are working on the incorporation and utilisation of the CB6-releasing trigger within more complex supramolecular systems, either in multicomponent mixtures or in an intramolecular manner.

Data availability

The data supporting this article have been included as part of the ESI.† Crystallographic data for compounds **6a**, **6b**, **6c**, and **6d** has been deposited at the Cambridge Crystallographic Data

Centre under respective numbers 2312915–2312918 and can be obtained from **https://www.ccdc.cam.ac.uk/structures**.

Author contributions

AZ and RV conceived and designed the experiments. All authors performed experiments and data analysis. RV wrote the draft with contributions from all co-authors. AZ, PJ, VK, JSW, ZP and MR prepared the initial version of ESI.† All authors reviewed and edited the draft and ESI.†

Conflicts of interest

There are no conflicts to declare.

Acknowledgements

The authors thank Professor Vladimír Šindelář from Masaryk University for valuable discussion over the manuscript. The financial support of this work by the Internal Funding Agency of Tomas Bata University in Zlín, project IGA/FT/2024/001, and the University of Jyväskylä is gratefully acknowledged.

Notes and references

1 (*a*) J.-X. Liu, K. Chen and C. Redshaw, *Chem. Soc. Rev.*, 2023, **52**, 1428–1455; (*b*) J. Yu, M. Gaedke and F. Schaufelberger, *Eur. J. Org Chem.*, 2023, **26**, e202201130; (*c*) M. Nandi, S. Bej, T. Jana and P. Ghosh, *Chem. Commun.*, 2023, **59**, 14776–14790; (*d*) N. Pearce, M. Tarnowska, N. J. Andersen, A. Wahrhafting-Lewis, B. S. Pilgrim and N. R. Champness, *Chem. Sci.*, 2022, **13**, 3915–3941; (*e*) A. W. Heard and S. M. Goldup, *ACS Cent. Sci.*, 2020, **6**, 117–128; (*f*) D. Sluysmans and J. F. Stoddart, *Trends Chem.*, 2019, **1**, 185–197.

2 (*a*) H. Y. Au-Yeung and Y. Deng, *Chem. Sci.*, 2022, **13**, 3315–3334; (*b*) J. Webb, *J. Am. Chem. Soc.*, 2020, **142**, 18859–18865; (*c*) J. J. Danon, D. A. Leigh, S. Pisano, A. Valero and I. J. Vitorica-Yrezabal, *Angew. Chem., Int. Ed.*, 2018, **57**, 13833–13837.

3 (*a*) Z. Ashbridge, S. D. P. Fielden, D. A. Leigh, L. Pirvu, F. Schaufelberger and L. Zhang, *Chem. Soc. Rev.*, 2022, **51**, 7779–7809; (*b*) D. H. Kim, N. Singh, J. Oh, E.-H. Kim, J. Juang, H. Kim and K.-W. Chi, *Angew. Chem., Int. Ed.*, 2018, **57**, 5669–5673; (*c*) D. A. Leigh, J. J. Danon, S. D. P. Fielden, J.-F. Lemonnier, G. F. S. Whitehead and S. L. Woltering, *Nat. Chem.*, 2021, **13**, 117–122; (*d*) D. A. Leigh, F. Schaufelberger, L. Pirvu, J. H. Stenlid, D. P. August and J. Segard, *Nature*, 2020, **584**, 562–568.

4 (*a*) Y. Lu, Y.-X. Deng, Y.-J. Lin, Y.-F. Han, L.-H. Weng, Z.-H. Li and G.-X. Jin, *Chem*, 2017, **3**, 110–121; (*b*) Y. Lu, P. D. Dutsche, J. Kinas, A. Hepp, G.-X. Jin and F. E. Hahn, *Angew. Chem., Int. Ed.*, 2023, **62**, e202217681.

5 (*a*) H. Xu, M.-D. Lin, J. Yuan, B. Zhou, Y. Mu, Y. Huo and K. Zhu, *Chem. Commun.*, 2021, **57**, 3239–3242; (*b*) X.-Y. Chen, D. Shen, K. Cai, Y. Jiao, H. Wu, B. Song, L. Zhang, Y. Tan, Y. Wang, Y. Feng, C. L. Stern and J. F. Stoddart, *J. Am. Chem. Soc.*, 2020, **142**, 20152–20160; (*c*) W. Liu, C. L. Stern and J. F. Stoddart, *J. Am. Chem. Soc.*, 2020, **142**, 10273–10278; (*d*) T.-H. Chiang, C.-Y. Tsou, Y.-H. Chang, C.-C. Lai, R. P. Cheng and S.-H. Chiu, *Org. Lett.*, 2021, **23**, 5787–5792.

6 I. T. Harrison and S. Harrison, *J. Am. Chem. Soc.*, 1967, **89**, 5723–5724.

7 (*a*) P. Wu, B. Dharmadhikari, P. Patra and X. Xiong, *Nanoscale Adv.*, 2022, **4**, 3418–3461; (*b*) L. Zhang, V. Marcos and D. A. Leigh, *Proc. Natl. Acad. Sci. U.S.A.*, 2018, **115**, 9397–9404; (*c*) L. Binks, S. Borsley, T. R. Gingrich, D. A. Leigh, E. Penocchio and B. M. W. Roberts, *Chem*, 2023, **9**, 2902–2917; (*d*) E. Moulin, L. Faour, C. C. Carmona-Vargas and N. Giuseppone, *Adv. Mater.*, 2019, **32**, 1906036.

8 (*a*) D. A. Leigh, V. Marcos and M. R. Wilson, *ACS Catal.*, 2014, **4**, 4490–4497; (*b*) C. Kwamen and J. Niemeyer, *Chem.–Eur. J.*, 2021, **27**, 175–186; (*c*) A. Martinez-Cuezva, A. Saura-Sanmartin, M. Alajarin and J. Berna, *ACS Catal.*, 2020, **10**, 7719–7733.

9 A. Saura-Sanmartin, *Beilstein J. Org. Chem.*, 2023, **19**, 873–880.

10 (*a*) F. d'Orchymont and J. P. Holland, *Chem. Sci.*, 2022, **13**, 12713–12725; (*b*) A. Fernandes, A. Viterisi, F. Coutrot, S. Potok, D. A. Leigh, V. Aucagne and S. Papot, *Angew. Chem., Int. Ed.*, 2009, **48**, 6443–6447; (*c*) R. Barat, T. Legigan, I. Tranoy-Opalinski, B. Renoux, E. Péraudeau, J. Clarhaut, P. Poinot, A. E. Fernandes, V. Aucagne, D. A. Leigh and S. Papot, *Chem. Sci.*, 2015, **6**, 2608–2613.

11 J. E. Green, J. W. Choi, A. Boukai, Y. Bunimovich, E. Johnston-Halperin, E. DeIonno, Y. Luo, B. A. Sheriff, K. Xu, Y. S. Shin, H.-R. Tseng, J. F. Stoddart and J. R. Heath, *Nature*, 2007, **445**, 414–417.

12 M. Xue, Y. Yang, X. Chi, X. Yan and F. Huang, *Chem. Rev.*, 2015, **115**, 7398–7501.

13 (*a*) X. Ling, E. L. Samuel, D. L. Patchell and E. Masson, *Org. Lett.*, 2010, **12**, 2730–2733; (*b*) A. C. Catalán and J. Tiburcio, *Chem. Commun.*, 2016, **52**, 9526–9529; (*c*) A. J. McConnell and P. D. Beer, *Chem.–Eur. J.*, 2011, **17**, 2724–2733; (*d*) H. Masai, J. Terao, T. Fujihara and Y. Tsuji, *Chem.–Eur. J.*, 2016, **22**, 6624–6630.

14 (*a*) A. H. G. David, P. García-Cerezo, A. G. Campaña, F. Santoyo-González and V. Blanco, *Chem.–Eur. J.*, 2019, **25**, 6170–6179; (*b*) M. A. Soto and M. J. MacLachlan, *Org. Lett.*, 2019, **21**, 1744–1748; (*c*) M. D. Cornelissen, S. Pilon, L. Steemers, M. J. Wanner, S. Frölke, E. Zuidinga, S. I. Jørgensen, J. I. van der Vlugt and J. H. van Maarseveen, *J. Org. Chem.*, 2020, **85**, 3146–3159; (*d*) P. Branná, M. Rouchal, Z. Prucková, L. Dastychová, R. Lenobel, T. Pospíšil, K. Maláč and R. Vícha, *Chem.–Eur. J.*, 2015, **21**, 11712–11718; (*e*) H.-L. Sun, H.-Y. Zhang, Z. Dai, X. Han and Y. Liu, *Chem.–Asian J.*, 2017, **12**, 265–270.

15 (*a*) M. Horn, J. Ihringer, P. T. Glink and J. F. Stoddart, *Chem.–Eur. J.*, 2003, **9**, 4046–4054; (*b*) J. Yin, S. Dasgupta and J. Wu, *Org. Lett.*, 2010, **12**, 1712–1715.

16 (*a*) I. Yoon, M. Narita, T. Shimizu and M. Asakawa, *J. Am. Chem. Soc.*, 2004, **126**, 16740–16741; (*b*) S.-Y. Hsueh,

J.-L. Ko, C.-C. Lai, Y.-H. Liu, S.-M. Peng and S.-H. Chiu, *Angew. Chem., Int. Ed.*, 2011, **48**, 6643–6646.

17 (*a*) C.-W. Chiu, C.-C. Lai and S.-H. Chiu, *J. Am. Chem. Soc.*, 2007, **129**, 3500–3501; (*b*) K. Fujimura, Y. Ueda, Y. Yamaoka, K. Takasu and T. Kawabata, *Angew. Chem., Int. Ed.*, 2023, **62**, e202303078.

18 (*a*) M. Denis and S. M. Goldup, *Nat. Rev. Chem*, 2017, **1**, 0061; (*b*) R. Jamagne, M. J. Power, Z.-H. Zhang, G. Zango, B. Gibber and D. A. Leigh, *Chem. Soc. Rev.*, 2024, **53**, 10216–10252.

19 C. J. Bruns and J. F. Stoddart, *The Nature of the Mechanical Bond: From Molecules to Machines*, John Wiley & Sons, Hoboken, NJ, 2016.

20 (*a*) D. Tomas, D. J. Tetlow, Y. Ren, S. Kassem, U. Karaca and D. A. Leigh, *Nat. Nanotechnol.*, 2022, **17**, 701–707; (*b*) L. Feng, Y. Qiu, Q.-H. Guo, Z. Chen, J. S. W. Seale, K. He, H. Wu, Y. Feng, O. Farha, R. D. Astumian and J. F. Stoddart, *Science*, 2021, **374**, 1215–1221; (*c*) Y. Ren, R. Jamagne, D. J. Tetlow and D. A. Leigh, *Nature*, 2022, **612**, 78–82; (*d*) Q.-H. Guo, Y. Qiu, X. Kuang, J. Liang, Y. Feng, L. Zhang, Y. Jiao, D. Shen, R. D. Astumian and J. F. Stoddart, *J. Am. Chem. Soc.*, 2020, **142**, 14443–14449; (*e*) T. Kench, P. A. Summers, M. K. Kuimova, J. E. M. Lewis and R. Vilar, *Angew. Chem., Int. Ed.*, 2021, **60**, 10928–10934; (*f*) C. C. Slack, J. A. Finbloom, K. Jeong, C. J. Bruns, D. E. Wemmer, A. Pines and M. B. Francis, *Chem. Commun.*, 2017, **53**, 1076–1079; (*g*) A. Tamura and N. Yui, *Polym. J.*, 2017, **49**, 527–534; (*h*) A. H. G. David, P. García-Cerezo, A. G. Campaña, F. Santoyo-González and V. Blanco, *Org. Chem. Front.*, 2022, **9**, 633–642; (*i*) S. C. Rajappan, D. R. McCarthy, J. P. Campbell, J. B. Ferrell, M. Sharafi, O. Ambrozaite, J. Li and S. T. Schneebeli, *Angew. Chem., Int. Ed.*, 2020, **59**, 16668–16674; (*j*) M. Zhang and G. De Bo, *J. Am. Chem. Soc.*, 2019, **141**, 15879–15883.

21 T. Muramatsu, Y. Okado, H. Traeger, S. Schrettl, N. Tamaoki, C. Weder and Y. Sagara, *J. Am. Chem. Soc.*, 2021, **143**, 9884–9892.

22 D. A. Leigh, L. Pirvu, F. Schaufelberger, D. J. Tetlow and L. Zhang, *Angew. Chem., Int. Ed.*, 2018, **57**, 10484–10488.

23 K.-D. Zhang, X. Zhao, G.-T. Wang, Y. Liu, Y. Zhang, H.-J. Lu, X.-K. Jiang and Z.-T. Li, *Angew. Chem., Int. Ed.*, 2011, **50**, 9866–9870.

24 Y. Sakata, R. Nakamura, T. Hibi and S. Akine, *Angew. Chem., Int. Ed.*, 2023, **62**, e202217048.

25 R. Djemili, S. Adrouche, S. Durot and V. Heitz, *J. Org. Chem.*, 2023, **88**, 14760–14766.

26 (*a*) A. Kermagoret and D. Bardelang, *Chem.–Eur. J.*, 2023, **29**, e202302114; (*b*) K. A. Assaf and W. M. Nau, *Chem. Soc. Rev.*, 2015, **44**, 394–418; (*c*) S. J. Barrow, S. Kasera, M. J. Rowland, J. del Barrio and O. A. Scherman, *Chem. Rev.*, 2015, **115**, 12320–12406.

27 (*a*) W. L. Mock and N. Y. Shih, *J. Org. Chem.*, 1983, **48**, 3618–3619; (*b*) M. V. Rekharsky, Y. H. Ko, N. Selvapalam, K. Kim and Y. Inoue, *Supramol. Chem.*, 2007, **19**, 39–46.

28 (*a*) P. Branná, J. Černochová, M. Rouchal, P. Kulhánek, M. Babinský, R. Marek, M. Nečas, I. Kuřitka and R. Vícha, *J. Org. Chem.*, 2016, **81**, 9595–9604; (*b*) M. K. Sinha, O. Reany, M. Yefet, M. Botoshansky and E. Keinan, *Chem.–Eur. J.*, 2012, **18**, 5589–5605; (*c*) Y.-C. Liu, W. M. Nau and A. Hennig, *Chem. Commun.*, 2019, **55**, 14123–14126.

29 J. Tomeček, A. Čablová, A. Hromádková, J. Novotný, R. Marek, I. Durník, P. Kulhánek, Z. Prucková, M. Rouchal, L. Dastychová and R. Vícha, *J. Org. Chem.*, 2021, **86**, 4483–4496.

30 Deposition numbers 2312915 (for **6a**), 2312916 (for **6b**), 2312917 (for **6c**), and 2312918 (for **6d**) contain the supplementary crystallographic data for this paper.

31 (*a*) C. Bannwarth, E. Caldeweyher, S. Ehlert, A. Hansen, P. Pracht, J. Seibert, S. Spicher and S. Grimme, *Wiley Interdiscip. Rev.: Comput. Mol. Sci.*, 2021, **11**, e01493; (*b*) C. Bannwarth, S. Ehlert and S. Grimme, *J. Chem. Theory Comput.*, 2019, **15**, 1652–1671.

32 (*a*) L. Yuan, R. Wang and D. H. Macartney, *J. Org. Chem.*, 2007, **72**, 4539–4542; (*b*) I. W. Wyman and D. H. Macartney, *J. Org. Chem.*, 2009, **74**, 8031–8038.

33 M. V. Rekharsky, T. Mori, C. Yang, Y. H. Ko, N. Selvapalam, H. Kim, D. Sobransingh, A. E. Kaifer, S. Liu, L. Isaacs, W. Chen, S. Moghaddam, M. K. Gilson, K. Kim and Y. Inoue, *Proc. Natl. Acad. Sci. U.S.A.*, 2007, **104**, 20737–20742.

34 (*a*) I. Neira, M. D. García, C. Peinador and A. E. Kaifer, *J. Org. Chem.*, 2019, **84**, 2325–2329; (*b*) S. Senler, B. Cheng and A. E. Kaifer, *Org. Lett.*, 2014, **16**, 5834–5837; (*c*) M. H. Tootoonchi, S. Yi and A. E. Kaifer, *J. Am. Chem. Soc.*, 2013, **135**, 10804–10809; (*d*) X. Ling and E. Masson, *Org. Lett.*, 2012, **14**, 4866–4869; (*e*) E. Masson, X. Lu, X. Ling and D. L. Patchell, *Org. Lett.*, 2009, **11**, 3798–3801; (*f*) G. Celtek, M. Artar, O. A. Scherman and D. Tuncel, *Chem.–Eur. J.*, 2009, **15**, 10360–10363; (*g*) P. Mukhopadhyay, P. Y. Zavalij and L. Isaacs, *J. Am. Chem. Soc.*, 2006, **128**, 14093–14102.